Thermoreversible Cylinder−Sphere Transition of Polystyrene-*block*-polyisoprene Diblock Copolymers in Dioctyl Phthalate Solutions

Shinichi Sakurai*,† and Takeji Hashimoto*

Department of Polymer Chemistry, Graduate School of Engineering, Kyoto University, Sakyo-ku, Kyoto 606-01, Japan

Lewis J. Fetters

Exxon Research and Engineering Company, Corporate Research Laboratories, Annandale, New Jersey 08801

Received February 27, 1995; Revised Manuscript Received October 18, 1995[⊗]

ABSTRACT: We present experimental results of a thermoreversible morphological transition between spheres and cylinders for polystyrene-*block*-polyisoprene diblock copolymers (SI) in dioctyl phthalate solutions. Morphologies were characterized using small-angle X-ray scattering (SAXS), and spherical and cylindrical states were found above and below the order−order transition (OOT) temperature, T_{OOT}, respectively. T_{OOT} increased with an increase of polymer concentration for the range covered in this study (higher than 70 wt % polymer concentration). The concentration dependence of T_{OOT} was found to be given by the relationship of $(\chi_{eff}r_C)_{OOT}/\phi_p r_C = A + B/T_{OOT}$, where $(\chi_{eff}r_C)_{OOT}$ denotes the critical value of the product of χ_{eff} and r_C at the cylinder−sphere OOT, χ_{eff} is the effective interaction parameter between styrene and isoprene segments in the presence of solvent, r_C is the reduced degree of polymerization of an entire block copolymer, and ϕ_p is the volume fraction of the block copolymer in the solution. A and B are constants characterizing the temperature dependence of the segmental interaction parameter χ_{SI} in bulk, where $A = -0.0258$ and $B = 27.9$ were evaluated by analyzing SAXS profiles from the disordered state. The critical values$(\chi_{eff}r_C)_{OOT} = 38.4$ for the cylinder−sphere transition and $30.5 \leq (\chi_{eff}r_C)_{ODT} \leq 32.3$ for the order−disorder transition (ODT) were determined from our experimental result on the ϕ_p dependence of T_{OOT} and that of T_{ODT}, respectively. These critical values were compared to the results of some theoretical studies. The SAXS measurements revealed thermoreversibility of the cylinder−sphere transition between 110 and 120 °C for an 80 wt % solution.

Introduction

Block copolymers exhibit a rich variety of morphology in a microphase-separated state (or ordered state). Recently, noteworthy developments in both experiments[1−6] and theories[7−13] have been accomplished for the morphology and for the phase transition between different morphological states. Therefore, the studies of morphology in block copolymers are still fascinating and stimulating, although the field itself was originated more than 20 years ago.[14,15] It is only recently that the signature of the thermoreversible order−order transition (OOT) has been observed experimentally.[1−6] We first reported signature of the thermoreversible cylinder−sphere transition for polystyrene-*block*-polyisoprene (SI) diblock copolymers in dioctyl phthalate (DOP) solutions in 1991 using the small-angle X-ray scattering (SAXS) technique.[1] Subsequently in 1992 Almdal et al.[2] reported the thermotropic OOT from cylinders to lamellae via new morphologies other than the ordinary spherical, cylindrical, and lamellar structures in the weak-segregation limit (WSL) regime, i.e., the regime close to the order−disorder transition (ODT). They have discussed the complexity of new morphologies in block copolymers.[5] They applied shearing to align cylinders and determined the new morphologies using two-dimensional small-angle neutron scattering patterns for poly(ethylene-*alt*-propylene)-*block*-poly(1-butene) diblock copolymers. We reported cylinder−sphere transition in SI melts using SAXS and transmission electron microscopy (TEM) in 1993.[3,4] Hajduk et al.[6] reported the thermoreversible morphology transition between cylinders and lamellae for polystyrene-*block*-poly(ethene-butene random copolymer) diblock copolymer melts in 1994.

Theoretical studies to examine thermodynamically stable morphologies were originated by the pioneering work of Helfand and Wassermann,[16] where their results are applicable to the strong-segregation limit (SSL) regime far below the ODT. The work of Semenov[17] and that of Ohta and Kawasaki[18] belong to the category of SSL theories. Although the thermotropic OOT has been experimentally observed, none of those SSL theories predicts such behavior. Since Leibler[19] constructed a morphological phase diagram for diblock copolymers at the WSL in 1980, further theoretical elaborations were devoted by Fredrickson and Helfand,[20] and Mayes and Olvera de la Cruz,[21] in order to take into account the effects of the composition fluctuation in the context of WSL theories. Contrary to the SSL theories, the WSL theories[19−21] predict the thermoreversible OOT. However, the WSL theories are not sufficient for explaining all experimental results because the theories cannot predict any aspects observed in the SSL regime.[22] Therefore, we need a theory to describe appropriately the morphological states in an intermediate segregation regime between SSL and WSL regimes. In other words, the WSL theories should be modified to include the chain stretching effects.[23] Recently, the theoretical considerations for all degrees of segregation were reported by Melenkevitz and Muthukumar,[7] Whitmore

* To whom correspondence should be addressed.
† Present address: Department of Polymer Science and Engineering, Kyoto Institute of Technology, Matsugasaki, Sakyo-ku, Kyoto 606, Japan
⊗ Abstract published in *Advance ACS Abstracts,* December 1, 1995.

0024-9297/96/2229-0740$12.00/0

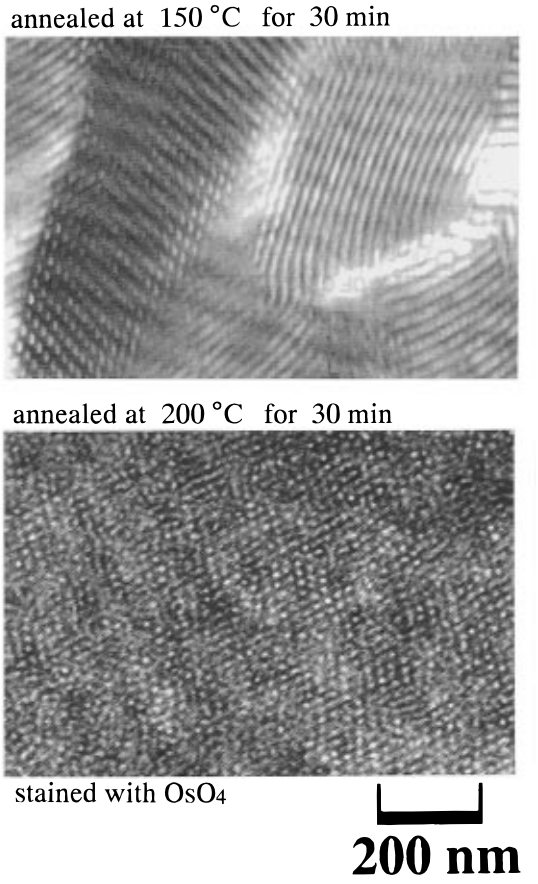

Figure 1. Transmission electron micrographs for the ultrathin-sections of bulk SI-16/82 samples annealed (a) at 150 °C for 30 min and (b) at 200 °C for 30 min. Dark and bright domains are OsO_4-stained PI domains and unstained PS domains, respectively.

and Vavasour[8−10], Shull,[11] Lescanec and Muthukumar,[12] and Muthukumar.[13] Melenkevitz and Muthukumar[7] used the density functional theory, and Whitmore and Vavasour[8] applied the self-consistent mean-field theory without assuming a narrow interface approximation. Vavasour and Whitmore[9] indicated that their result of the morphology phase diagram completely agrees with the Leibler's result in the WSL regime and agrees with the result of Helfand and Wassermann[16] in the SSL regime. Vavasour and Whitmore[10] further developed a theory which takes into account effects of chain asymmetry arising from differences in statistical segment length and segment volume. It is noteworthy that Muthukmar[13] further took into account effects of the composition fluctuation in diblock copolymers. Our experimental results will be compared to some of those theoretical results.

We have already reported thermoreversible cylinder−sphere OOT in SI diblock copolymer melts having the volume fraction of polystyrene (PS), $f_{PS} = 0.15$.[3,4] The clear signature of the thermoreversible cylinder−sphere OOT between 150 and 200 °C was obtained by observations of SAXS and TEM (see the following discussion and Figure 1).[3,4] Since it takes a long time for melt samples to attain thermodynamic equilibrium, one should carefully prepare samples in order to discuss thermodynamically equilibrium morphological structures. Moreover, one could experience experimental difficulty and inconvenience in the case of using melt samples. First of all, *in situ* SAXS measurements at equilibrium states are difficult at high temperatures because of possible thermal degradation of the samples. Secondly, one could not completely avoid the thermal degradation when the samples are further annealed at high temperatures in order to thoroughly check the stability of the morphological structures. Therefore, a more convenient way to study the OOT is required. Although we have to sacrifice merits of using melt samples, such as TEM observations, block copolymer solutions are more suitable for the OOT study in a sense that time required to attain equilibrium can be much reduced. Since for our particular SI melt sample we have already confirmed the thermoreversible cylinder−sphere transition by the TEM observation, the SAXS observations are satisfactory in order to check the transition for solutions of the same SI sample. We report in the present paper on the cylinder−sphere OOT for the SI/DOP solutions with 70 and 80 wt % polymer concentrations as revealed by *in situ* SAXS measurements at high temperatures. In the course of analysis, we assume neutrality of DOP for the SI diblock copolymers and dilution approximation[24,25] used to express the effective interaction parameter χ_{eff}, as a function of the polymer concentration ϕ_p, as $\chi_{eff} = \chi_{SI}\phi_p$. The phase diagram of thermodynamically stable morphology is discussed in terms of temperature and polymer concentration in the solution.

Experimental Section

The SI sample used (code name SI-16/82) has the number-average molecular weight, $M_n = 8.2 \times 10^4$ and the heterogeneity index, $M_w/M_n = 1.05$, where M_w designates the weight-average molecular weight. The weight fraction of PS, w_{PS}, is 0.16. The microstructures in the polyisoprene (PI) blocks are 93 and 7% for 1,4- and 3,4-linkages, respectively. The details of the synthesis and characterization were described elsewhere.[4,26] DOP was used as a solvent in the solution studies.

SAXS experiments were conducted at the edge-view geometry, according to the method described in detail elsewhere.[4,25,27] The cross-section of the incident X-ray beam is rectangular (so called slit collimation) and its long axis is set parallel to surfaces of a stack of film samples. The incident beam passes through the stack parallel to their surfaces, and a one-dimensional position-sensitive proportional counter was set parallel to the film normal to detect the scattered X-rays. Because the incident beam has finite area rather than point, the measured SAXS profile is smeared. This smearing effect should be corrected for by desmearing the measured SAXS profile. However, it is not possible to desmear the scattered pattern from an oriented system.[28] The purpose of the SAXS measurement is to characterize the morphological structures, and therefore information on the relative peak positions of the lattice scattering is merely needed. Note that the lattice scattering peaks are associated with spatial regularity and symmetry of the ordered domains. The error due to smearing does not affect the relationship of the lattice peak positions[27] for the collimation optics adopted in this work, so that we can use the measured (smeared) SAXS profiles for the characterization of morphology in the following discussion. The measured scattered intensities were corrected for absorption due to the sample, air scattering, thickness of the sample, and thermal diffuse scattering arising from density fluctuations.

Instead of using a conventional degree of polymerization, N ($= N_A + N_B$), it is convenient to define the reduced degree of polymerization of an entire block chain, r_C ($= r_A + r_B$), which is corrected for asymmetry in segment size. We define r_K for K component as:

$$r_K = (v_K/v_0)N_K \text{ (K = A or B)} \quad (1)$$

where v_A and v_B denote molar volumes of segment A and B, respectively, and v_0 designates a molar volume of reference cell. v_K is given by $M_{u,K}/\rho_K$, where $M_{u,K}$ is a molecular weight of the K segment and ρ_K is density of the K-polymer. We assume here $v_0 = (v_A v_B)^{1/2}$. Then the effective fraction (volume

fraction), f_K, is defined by

$$f_K = r_K/r_C = \nu_K N_K/(\nu_A N_A + \nu_B N_B) \quad (2)$$

For the SI-16/82 sample, $r_C = 1082$ and $f_{PS} = 0.14$ have been evaluated,[29] using $w_{PS} = 0.16$, $\rho_{PS} = 0.969$ g/cm^3 for PS at 413 K ($> T_{g,PS}$) and $\rho_{PI} = 0.830$ g/cm^3 for 1,4-polyisoprene at 413 K, respectively.[30]

Results and Discussion

First of all, let us discuss a morphological change for the bulk sample by changing temperature. Figure 1 displays TEM micrographs for the ultrathin-sections of bulk SI-16/82 samples annealed (a) at 150 °C for 30 min and (b) at 200 °C for 30 min. Dark and bright domains are OsO_4-stained PI domains and unstained PS domains, respectively. In part a, one can recognize hexagonal arrays of PS-cylinders because cross-sectional images parallel and perpendicular to cylinder axes are both observable in this micrograph. On the other hand, nearly circular PS-domains each having similar size are observed all over the image in part b. One can see regularity of spatial distribution of the PS-domains in some regions. Since this micrograph shows no rodlike image, we concluded that the morphology is spherical, although the packing symmetry of the spherical domains cannot be identified from this image alone in part b. Thus, Figure 1 shows a clear signature of the thermotropic morphological transition. The thermoreversibility of this cylinder−sphere transition for the bulk SI-16/82 samples was also confirmed in our previous study.[4]

Next, we discuss the morphological characterization using SAXS measurements. Note that the SAXS measurements were conducted at the edge-view geometry and the SAXS profiles were smeared by the slit collimation. The SAXS profiles for SI-16/82 solutions in DOP at 80 and 70 wt % polymer concentrations are shown in Figures 2 and 3, respectively. The volume fraction of polymer (ϕ_p) in the solutions were, respectively, 0.81 and 0.72. These profiles were measured via a stepwise increase in the sample temperature. The profiles are displayed in a semilogarithmic plot of the absolute scattered intensity vs the magnitude of the scattering vector, s, which is given by

$$s = \mathbf{s} = (2 \sin \theta)/\lambda \quad (3)$$

with θ and λ being half the scattering angle and the wavelength of X-rays with 0.154 nm, respectively. For the 80 wt % solution at 100 °C the scattering peaks were observed at s-values of 1, $\sqrt{3}$, and $\sqrt{4}$ relative to the first-order peak position. These are the lattice scattering peaks of hexagonally-packed cylinders, as expressed by $(h^2 + hk + k^2)^{1/2}$ with h, k = 0, 1, 2, 3, ... On the other hand, for the 80 wt % solution at 150 °C, the lattice scattering peaks are detected at relative s-values of $1{:}\sqrt{2}{:}\sqrt{3}{:}\sqrt{4}$. These are ascribed to the spherical microdomains arranged in a cubic lattice, as expressed by $\sqrt{n}$ with n = 1, 2, 3, ... As far as we know, all theories[7−13,16−21] predict the body-centered-cubic (bcc) lattice for the most stable lattice structure for spheres. Moreover, we have confirmed bcc lattice structures for this particular SI bulk sample at 200 °C using SAXS in our previous study.[4] Consequently, the SAXS results shown in Figure 2 indicate that the cylindrical microdomains were transformed into the spherical microdomains by raising the temperature. Similarly, the morphological states for the 70 wt % solution are found to be cylindrical and spherical at 90 and 100 °C, respectively.

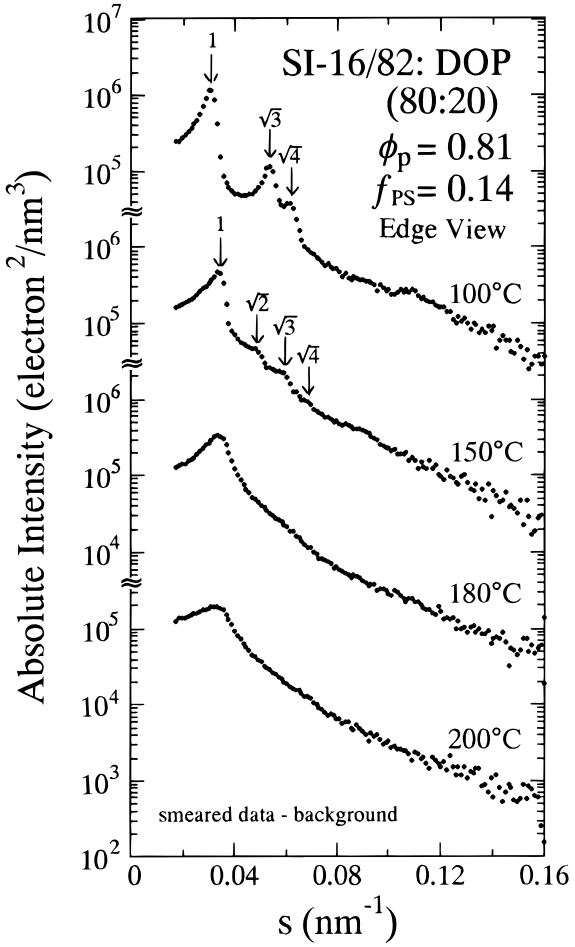

Figure 2. Smeared SAXS profiles for an 80 wt % solution of SI-16/82 in DOP (edge view).

For the 80 wt % solution at 180 and 200 °C and for the 70 wt % solution at 150, 180, and 200 °C, a single scattering peak was observed. Since the structure factor shows a single peak for the disordered block copolymer, we concluded that those solutions were at the disordered state; although our conclusion is not rigorous but is only an approximation. We also judge the onset of the disordered state for those solutions from temperature dependence of the first-order peak position s^*: in those SAXS profiles, s^* shows no temperature and concentration dependencies ($s^* = 0.033$ nm^{-1}). Note that those profiles used for the morphological characterization were measured upon the stepwise increase of the sample temperature. One can see that the regime showing no temperature and concentration dependencies of s^* may correspond to the disordered state. In a rigorous sense one should see weak temperature dependence of s^* because of thermal expansion of the polymer chains.[31] Also there is an issue for the variation of s^* with polymer concentration because of the swelling effect of solvent; Duplessix et al. reported a shift of s^* to higher values with an increase of polymer concentration for the experimental condition including the concentrated regime,[32] whereas Mayes et al.[33] found almost concentration-independent peak position s^* (as $s^* \sim \phi_p^{0.05}$) in the semidilute regime ($0.01 < \phi_p < 0.13$). Further discussion is beyond the scope of this study, and we conclude that the morphological state for the 80 wt % solution at $T \geq 180$ °C and for the 70 wt % solution at $T \geq 150$ °C is the disordered state.

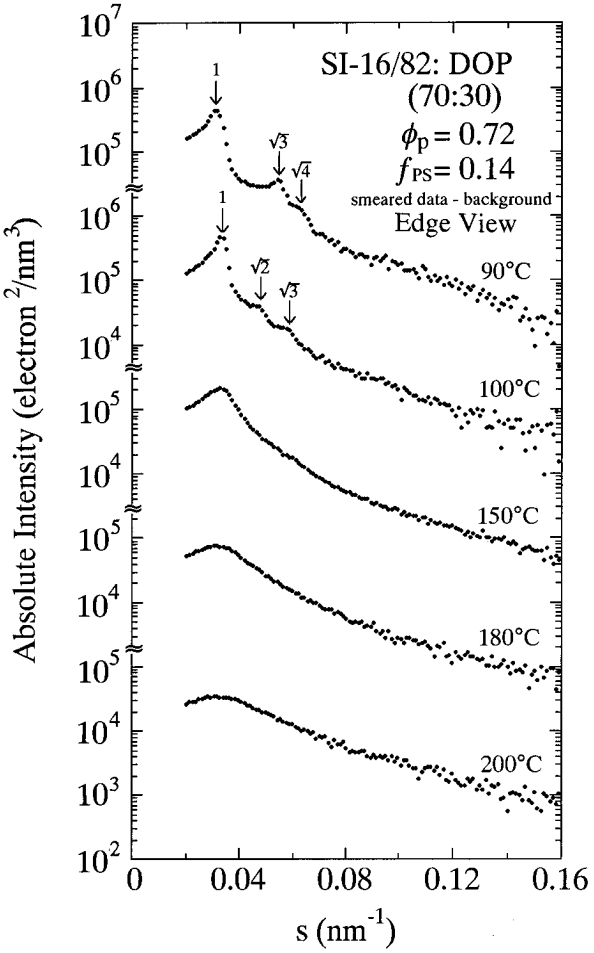

Figure 3. Smeared SAXS profiles for a 70 wt % solution of SI-16/82 in DOP (edge view).

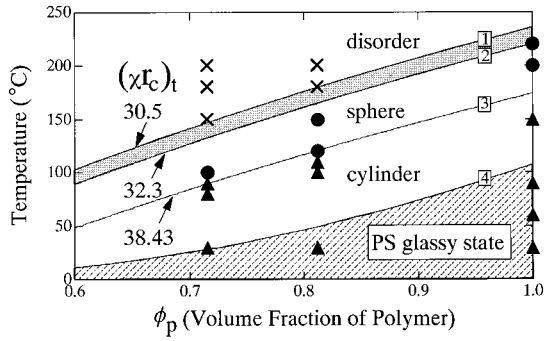

Figure 4. Temperature−ϕ_p plot showing morphological states analyzed by SAXS.

The observed morphological states are summarized in the plot of temperature vs ϕ_p in Figure 4. The hatching below the curve 4 indicates the region where thermodynamic equilibrium is hard to achieve due to vitrification of the PS domains. The border line (curve 4) for the hatching region was drawn based on the published result of the glass transition temperature of the PS domains in SI/toluene solutions as a function of polymer concentration.[34] For the 80 wt % solution, the cylinder-sphere transition took place between 110 and 120 °C. For the 70 wt % solution, it occurred between 90 and 100 °C. The disordered state is $T \geq 150$ °C for the 70 wt % solution and $T \geq 180$ °C for the 80 wt % solution. As definitely is seen, the transition temperatures T_{OOT} and T_{ODT} increase with an increase of polymer concentration. According to the following criteria, we determined the transition lines based on

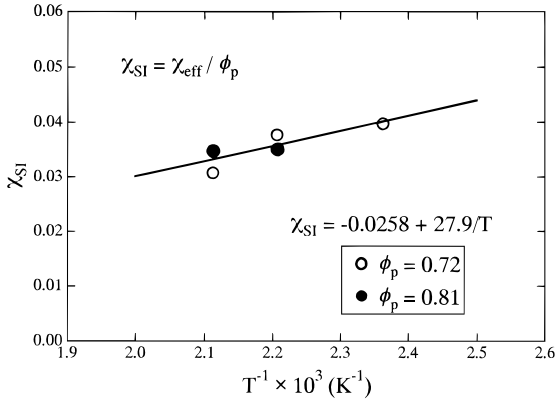

Figure 5. Plot of χ_{SI} vs inverse of the absolute temperature, T^{-1}.

temperature and concentration dependencies of the interaction parameter χ_{eff}. The morphological state can be correlated to the segregation power, and therefore the morphological transition can be discussed in terms of the product of an effective χ value in the solution (χ_{eff}) and r_C. At the order−disorder transition, we set $\chi_{eff}r_C = (\chi_{eff}r_C)_{ODT}$, where $(\chi_{eff}r_C)_{ODT}$ is the critical value of the product of χ_{eff} and r_C at the ODT. Similarly, $\chi_{eff}r_C = (\chi_{eff}r_C)_{OOT}$ leads the critical condition for the cylinder−sphere OOT. To express χ_{eff} as a function of ϕ_p, we assume the dilution approximation $\chi_{eff} = \chi_{SI}\phi_p$. Since the solutions examined in this study can be considered to be in the fully concentrated regime, the approximation of $\chi_{eff} = \chi_{SI}\phi_p$ is valid for our system. The neutrality of the solvent DOP is another issue of discussion. We will discuss this later on. Using the temperature dependence of χ_{SI} ($= A + B/T$), we eventually obtain the relationship of

$$\frac{(\chi_{eff}r_C)_t}{\phi_p r_C} = A + \frac{B}{T_t} \qquad \text{(t; ODT or OOT)} \qquad (4)$$

where A and B are constants defining the temperature dependence of χ_{SI} ($A = -0.0258$ and $B = 27.9$ in bulk; see the following paragraph and Figure 5). $(\chi_{eff}r_C)_t$ and T_t denote, respectively, the critical value of $\chi_{eff}r_C$ and the transition temperature for the ODT or OOT, where t designates ODT or OOT. The purpose of utilizing the eq 4 is to evaluate the critical values $(\chi_{eff}r_C)_t$ from our experimental results. The curves 1−3 in Figure 4 were drawn using eq 4 with $(\chi_{eff}r_C)_t$ values of 30.5, 32.3, and 38.43, respectively. The curve 1 goes through the point of ($T = 180$ °C, $\phi_p = 0.81$) where the solution was at the disordered state. One can see the disordered region and the spherical region above and below the curve 1, respectively. Therefore, the value 30.5 can be a candidate for the $(\chi_{eff}r_C)_{ODT}$. However, this is not the only one. Curve 2, which was drawn so as to go through the point of ($T = 220$ °C, $\phi_p = 1.0$) where the bulk sample showed spherical morphology, is another candidate for the phase boundary of the ODT. From our experimental results we can only state that the critical value for the ODT is in the range of $30.5 \leq (\chi_{eff}r_C)_{ODT} \leq 32.3$, and the true transition line for the ODT may be located in the shaded area between the curves 1 and 2. Curve 3 which approximately goes through both the point of ($T = 90$ °C, $\phi_p = 0.72$) and that of ($T = 120$ °C, $\phi_p = 0.81$) is appropriate for the cylinder−sphere OOT, giving $(\chi_{eff}r_C)_{OOT} = 38.43$.

Now we show the temperature dependence of χ_{SI}. The values of χ_{SI} were evaluated by analyzing the SAXS

Table 1. Comparison of the Experimental and Theoretical Results of $(\chi_{eff}r_C)_t$ (t; OOT or ODT)

	$(\chi_{eff}r_C)_t$	
	cylinder−sphere OOT	ODT
experimental results	38.4	30.5−32.3
theoretical results		
Leibler[19] (1980)	43.5	40.6
Vavasour & Whitmore[9] (1992)	72.2	32.1
Vavasour & Whitmore[10] (1993)	47.6	31.4
Lescanec & Muthukumar[12] (1993)	–	42.0
Muthukumar[13] (1993)	–	39.7

profiles from the disordered state. The method of the analysis is in principle the same as that reported before[25] which includes corrections for polydispersity, composition distribution, and effects of chain asymmetry on the scattering function. In order to evaluate bulk χ_{SI} values from the effective values (χ_{eff}), which were obtained for the solutions, the dilution approximation was used. As a result of the analysis of the SAXS profiles at 180 and 200 °C for the 80 wt % solution and at 150, 180, and 200 °C for the 70 wt % solution, the effective values χ_{eff} and resulting bulk χ_{SI} values were obtained. The plot of χ_{SI} vs inverse of the absolute temperature, T^{-1}, is shown in Figure 5. It is found that the temperature dependence of the evaluated χ_{SI} can be approximated by

$$\chi_{SI} = -0.0258 + \frac{27.9}{T} \quad (5)$$

This relationship was utilized in the determination of the transition lines (curves 1−3) drawn in Figure 4. The radius of gyration of the entire block copolymer, $R_{g,SI}$, was also determined by analyzing the SAXS profiles to be 9.4 nm, irrespective of temperature and polymer concentration. Using the following equation for SI diblock copolymers,

$$R^2_{g,SI} = \frac{N_{PS}b^2_{PS} + N_{PI}b^2_{PI}}{6} \quad (6)$$

we calculated $R_{g,SI} = 9.2$ nm from literature values[30] of the statistical segment lengths for PS and PI, respectively, $b_{PS} = 0.67$ nm and $b_{PI} = 0.65$ nm, at 413 K. The agreement of the values for $R_{g,SI}$ fortifies the validity of the method employed in this study to analyze the SAXS profiles from the disordered state.

We now compare our experimental results of the critical values $(\chi_{eff}r_C)_t$ with theoretical results. Table 1 is a list of values for the ODT and the cylinder−sphere OOT. The theories of Muthukumar et al.[12,13] do not predict the equilibrium cylindrical state for $f_{PS} = 0.14$ of our SI sample, irrespective of temperatures. Therefore, we compare our experimental results with the theoretical results of Leibler[19] and with those of Vavasour and Whitmore.[9,10] Our experimental results are $(\chi_{eff}r_C)_{OOT} = 38.4$ for the cylinder−sphere transition and $(\chi_{eff}r_C)_{ODT} = 30.5-32.3$ for the ODT. In comparison with Leibler's prediction,[19] the agreement is good for the cylinder−sphere transition but not good for the ODT. On the other hand, the results of Vavasour and Whitmore in 1993,[10] in which the effects of chain asymmetry was taken into account, are consistent with our results for the ODT but not very consistent for the cylinder−sphere transition. Further experimental examination should be required for a more quantitative comparison.

Finally we discuss thermoreversibility of the cylinder−sphere transition in the SI/DOP solution. In order to confirm the thermoreversibility, SAXS measurements with changing temperature up and down between 110 and 120 °C were conducted for the 80 wt % solution according to the diagram shown in Figure 6, where the measurements were done at the specified time-regions of A−D and 1−4. The SAXS profiles measured at A−D (shown in Figure 7) display transient changes of the structures induced by cooling down from 120 to 110 °C (SAXS profiles A to C) and by heating up from 110 to 120 °C (SAXS profile D). The SAXS profiles measured at 1−4 are shown in Figure 8 to display the thermoreversibility of the cylinder−sphere transition. Prior to discussing the thermoreversibility, we first confirm that the SAXS profiles obtained at 3 (110 °C) and 4 (120 °C) reflect the equilibrium states by examining the SAXS profiles measured at A−D shown in Figure 7. Upon cooling down from 120 to 110 °C, one can follow changes in the SAXS profiles from 2 to 3 via A, B, and C. Along with the change in the SAXS profiles from A to C at 110 °C, the $\sqrt{2}$ peak is becoming less intense, the $\sqrt{3}$ peak is getting sharper, and the $\sqrt{4}$ shoulder is appear-

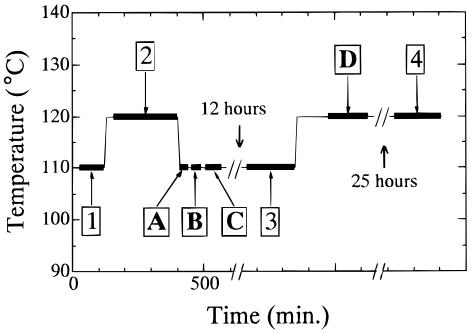

Figure 6. Thermal histories of the 80 wt % solution for the SAXS profiles shown in Figures 7 and 8.

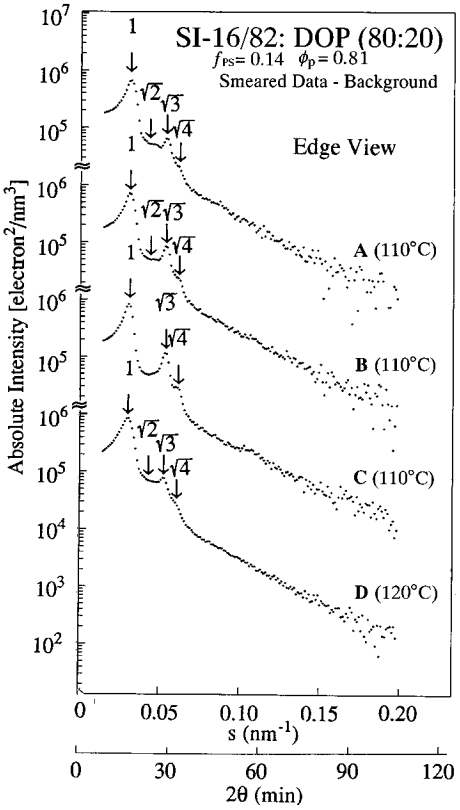

Figure 7. Smeared SAXS profiles (edge view) for the 80 wt % solutions at 110 and 120 °C. The profiles were measured at time-region indicated with A−D in Figure 6.

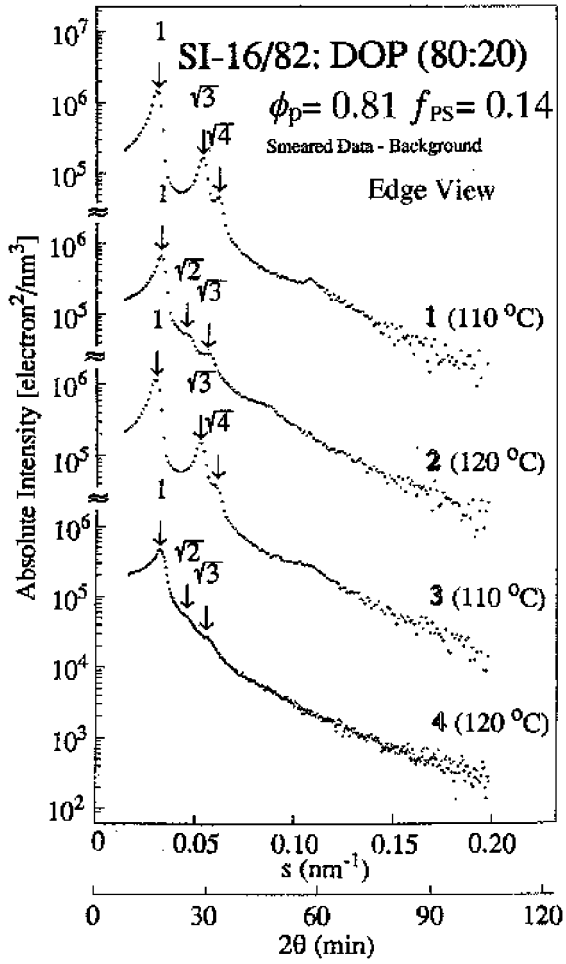

Figure 8. Smeared SAXS profiles (edge view) for the 80 wt % solutions at 110 and 120 °C. The profiles were measured at time-region indicated with 1−4 in Figure 6.

ing. The profiles A and B therefore appeared in the course of the transition from spheres to cylinders. On the other hand, the profile C indicates that the morphological structure has already reached equilibrium, because the profile C is identical to the profile 3 shown in Figure 8. Upon heating up from 110 to 120 °C, one can follow changes in the SAXS profiles from 3 to 4 via D. The profile D at 120 °C differs markedly from the profile 4 and is rather similar to the profile A at 110 °C, indicating that the morphological structure is formed in the course of the transition. Thus, upon cooling down from 120 to 110 °C and heating up from 110 to 120 °C, an annealing period longer than 1.4 h and that longer than 4.5 h were required, respectively, to equilibrate the morphological structures. Surprisingly such long annealing times are required even in the case of using solutions, and this indicates the difficulty in the study of thermoreversible OOT.

Figure 8 shows the SAXS profiles 1−4. The profiles 3 and 4 were measured after equilibrating the morphological structures by fully annealing the samples at 110 and 120 °C, respectively. Based on the same criteria of the morphology determination, the morphologies were cylindrical and spherical at 110 and 120 °C, respectively, irrespective of the thermal history of the solution. Thus, it can be concluded that the cylinder−sphere transition is thermoreversible. The interesting feature is that the position of the first-order peak does not change much along the transition, i.e., s = 0.032, 0.033, 0.031, and 0.032 nm^{-1} for 1, 2, 3, and 4, respectively. It should be noted that we reported in our previous study[4] the position of the first-order peak changed very much for the samples annealed at 150 and 200 °C, for which the morphologies were cylinders and spheres, respectively. Since in the previous study we used samples quenched to 0 °C from the annealing temperature of 150 or 200 °C in order to conduct the SAXS measurements at the room temperature, it was not possible to precisely specify the temperature at which the morphological state was frozen in. On the other hand, we are sure that the SAXS results shown in Figure 8 are at the thermodynamically equilibrium state. In a rigorous sense, the temperature difference between 110 and 120 °C may cause a little change in the peak position due to change of interaction parameter,[35] as $s = d^{-1} \sim \chi_{eff}^{-1/3}$. Then the ratio s(120 °C)/s(110 °C) can be estimated from the effective χ value using eq 5 with the dilution approximation: s(120 °C)/s(110 °C) $\sim$ [χ_{eff}(120 °C)/χ_{eff}(110 °C)]$^{-1/3} \sim$ 1.013. The experimental result leads to 1.03 for the ratio s(120 °C)/s(110 °C), which is still larger than that due to the effect of temperature difference between 110 and 120 °C. However, the deviation in the peak position, if it is corrected for the effect of temperature dependence, is within the experimental error of ±0.001 nm^{-1} in s.

The values of the Bragg spacing d evaluated from the position of the first-order lattice scattering peak are 3.2, 3.1, 3.3, and 3.1 nm for 1, 2, 3, and 4, respectively. On the basis of this result, we can consider a scheme how spheres coalesce each other to form cylinders. Noting that the Bragg spacing giving rise to the first-order lattice scattering peak is the spacing of (110) plane for the bcc-spheres and that is the spacing of (100) plane for the hex-cylinders, the experimental result is expressed by d_{110}(bcc) = d_{100}(hex). Figure 9a illustrates a unit cell of bcc-spheres, where three black spheres are placed on a (111) plane shown with thin solid lines, three hatched spheres are on another (111) plane shown with thick broken lines, and three white spheres, with the nearest neighbor distances, are placed linearly in a direction normal to (111) planes. One can find that a distance between two of those black spheres is identical to $2d_{110}$(bcc), as indicated in Figure 9a. Since the view from the direction normal to a (111) plane (from the thick arrow shown in Figure 9a) is hexagonal as illustrated in Figure 9b, a coalescence of the neighboring spheres in the direction normal to a (111) plane forms hex-cylinders as illustrated in Figure 9d which is the view of hex-cylinders in Figure 9c from the direction parallel to the cylinder axes. Our experimental result of d_{110}(bcc) = d_{100}(hex) indicates that the position of the center of mass for the spheres remains unchanged upon coalescence. In order to meet this requirement, a possible transition scheme may accompany the stretching of spheres along the direction normal to a (111) plane. Here we mainly consider the coalescence of the neighboring spheres induced by a curvature change of the interface from a sphere to a prolate spheroid with its long axis oriented normal to the (111) plane. The radius of thus formed cylinder should be smaller than that of sphere, i.e., $R_{sph} > R_{cyl}$, as shown in Figure 9. For the cylinder-to-sphere transition, the reverse mechanism for a pinching off from cylinders to spheres may be reasonable in order to meet d_{110}(bcc) = d_{100}(hex) and this mechanism may accompany necked cylinders having the undulating interfaces.[36] Although the transition scheme accompanying undulation of the interfaces was presented also for the cylinder-to-lamellar transition in our previous

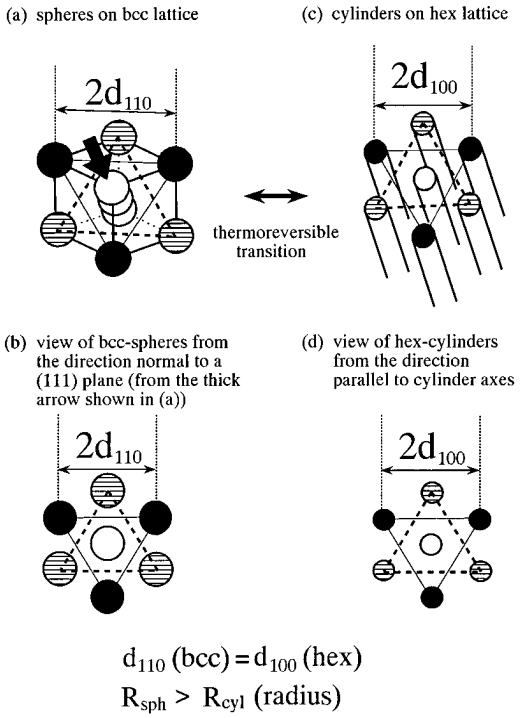

Figure 9. (a) Unit cell of body-centered-cubic (bcc) spheres, (b) view of bcc-spheres from the direction normal to a (111) plane (from the thick arrow shown in (a)), (c) array of hexagonal (hex) cylinders, and (d) view of hex-cylinders from the direction parallel to the cylinder axes. The Bragg spacing giving rise to the first order lattice scattering peak is the spacing of (110) plane for the bcc-spheres and that is the spacing of (100) plane for the hex-cylinders. Note that the position of the first-order peak does not change along the transition as seen in Figure 8. To meet this requirement of d_{110}(bcc) = d_{100}(hex), the sphere−cylinder transition should accompany an elongation of spheres into prolate spheroids oriented normal to the (111) plane and a coalescence as shown in the change from a to c.

study,[27] we cannot say that the OOT is always governed by the interfacial deformation, because Hajduk et al.[6] presented an alternative mechanism mainly governed by movement of cylinders in the event of the thermoreversible OOT between cylinders and lamellae. Direct TEM observation is needed to confirm the presence of the undulating interfaces.

Conclusions

Thermoreversible morphological transition between spheres and cylinders has been studied using SAXS for SI diblock copolymers in DOP solutions. The morphologies are spheres and cylinders above and below the transition temperature, T_{OOT}, respectively. T_{OOT} increased with an increase of polymer concentration in the range covered in this study (higher than 70 wt % polymer concentration). The concentration dependence of T_{OOT} was found to be given by the relationship of $(\chi_{eff}r_C)_{OOT}/\phi_p r_C = A + B/T_{OOT}$. Here we assume the dilution approximation in order to express the effective interaction parameter χ_{eff} as a function of the polymer concentration ϕ_p, $\chi_{eff} = \chi_{SI}\phi_p$. A and B are constants defining the temperature dependence of χ_{SI}, and $A = -0.0258$ and $B = 27.9$ were evaluated by analyzing SAXS profiles from the disordered state. The critical values $(\chi_{eff}r_C)_{OOT} = 38.4$ for the cylinder−sphere transition and $(\chi_{eff}r_C)_{ODT} = 30.5-32.3$ for the order−disorder transition were determined from our experimental result on the ϕ_p dependence of T_{OOT} and that of T_{ODT}, respectively. These critical values were compared to some theoretical results. Although the recent theoretical study of Vavasour and Whitmore,[10] which is applicable to all degrees of segregation and includes effects of chain asymmetry, describes our experimental results, further experimental examination is required for quantitative comparison.

The SAXS measurements revealed thermoreversibility of the cylinder−sphere transition for the 80 wt % solution at 110 and 120 °C. The interesting feature is that the position of the first-order peak does not change along the transition, indicating that d_{110} of bcc-sphere is identical to d_{100} of hex-cylinders. A possible scheme proposed for the sphere-to-cylinder transition is the coalescence of the neighboring spheres in the direction normal to a (111) plane with deformation of spheres into prolate spheroids. For the cylinder-to-sphere transition, the reverse mechanism for a pinching off from cylinders to spheres may be in play. This meets the requirement that d_{110}(bcc) = d_{100}(hex) and this mechanism may accompany necked cylinders having the undulating interfaces. Direct TEM observation is needed to reveal the mechanism for the cylinder−sphere transition.

References and Notes

(1) Sakurai, S.; Hashimoto, T.; Fetters, L. J. *Polym. Prepr., Jpn., Soc. Polym. Sci., Jpn.* **1991**, *40*(*3*), 770.
(2) Almdal, K.; Koppi, K. A.; Bates, F. S.; Mortensen, K. *Macromolecules* **1992**, *25*, 1743.
(3) Sakurai, S.; Kawada, H.; Hashimoto, T.; Fetters, L. J. *Proc. Jpn. Acad.* **1993**, *69* (*Ser. B*), 13.
(4) Sakurai, S.; Kawada, H.; Hashimoto, T.; Fetters, L. J. *Macromolecules* **1993**, *26*, 5796.
(5) Hamley, I. W.; Koppi, K. A.; Rosedale, J. H.; Bates, F. S.; Almdal, K.; Mortensen, K. *Macromolecules* **1993**, *26*, 5959: Foerster, S.; Khandpur, A. K.; Zhao, J.; Bates, F. S.; Hamley, I. W.; Ryan, A. J.; Bras, W. *Macromolecules* **1994**, *27*, 6922.
(6) Hajduk, D. A.; Gruner, S. M.; Rangarajan, P.; Register, R. A.; Fetters, L. J.; Honeker, C.; Albalak, R. J.; Thomas, E. L. *Macromolecules* **1994**, *27*, 490.
(7) Melenkevitz, J.; Muthukumar, M. *Macromolecules* **1991**, *24*, 4199.
(8) Whitmore, M. D.; Vavasour, J. D. *Macromolecules* **1992**, *25*, 2041.
(9) Vavasour, J. D.; Whitmore, M. D. *Macromolecules* **1992**, *25*, 5477.
(10) Vavasour, J. D.; Whitmore, M. D. *Macromolecules* **1993**, *26*, 7070.
(11) Shull, K. R. *Macromolecules* **1992**, *25*, 2122.
(12) Lescanec, R. L.; Muthukumar, M. *Macromolecules* **1993**, *26*, 3908.
(13) Muthukumar, M. *Macromolecules* **1993**, *26*, 5259.
(14) Molau, G. E. In *Block Polymers*; Aggarwal, S. L., Ed., 1970; Plenum Press: New York, pp 79−106.
(15) Aggarwal, S. L. *Polymer* **1976**, *17*, 938.
(16) For example, see Helfand, E.; Wassermann, Z. R. In *Developments in Block Copolymers-1*; Goodman, I., Ed.; Applied Science Publishers: Oxford, UK, 1982; chap 4, pp 99−125.
(17) Semenov, A. N. *JETP Lett.* (*Engl. Transl.*) **1985**, *61*, 733.
(18) Ohta, T.; Kawasaki, K. *Macromolecules* **1986**, *19*, 2621.
(19) Leibler, L. *Macromolecules* **1980**, *13*, 1602.
(20) Fredrickson, G. H.; Helfand, E. *J. Chem. Phys.* **1987**, *87*, 697.
(21) Mayes, A. M.; Olvera de la Cruz, M. *J. Chem. Phys.* **1991**, *95*, 4670.
(22) Hasegawa, H.; Tanaka, H.; Yamasaki, K.; Hashimoto, T. *Macromolecules* **1987**, *20*, 1651.
(23) The stretching of a block copolymer chain in the disordered state near ODT was first clearly observed and pointed out by Owens et al.[37] Bates and Fredrickson[38] and Sakurai et al.[4] pointed out that the effects of the chain stretching on the OOT should also be taken into account in the theories for comparisons with the experimental results.
(24) Hashimoto, T.; Mori, K. *Macromolecules* **1990**, *23*, 5347.
(25) Sakurai, S.; Mori, K.; Okawara, A.; Kimishima, K.; Hashimoto, T. *Macromolecules* **1992**, *25*, 2679.
(26) Morton, M.; Fetters, L. J. *Rubb. Chem. Tech.* **1975**, *48*, 359.
(27) Sakurai, S.; Momii, T.; Taie, K.; Shibayama, M.; Nomura, S.; Hashimoto, T. *Macromolecules* **1993**, *26*, 485.

(28) Stein, R. S.; Wilkes, G. L. In *Structure and Properties of Oriented Polymers*; Ward, I. M., Ed.; Applied Science Publishers Ltd.: London, 1975; Chap. 3.

(29) In order to calculate the degree of polymerization, N_K for K = A or B, the equation $N_K = M_w \times w_K/M_{u,K}$ should be used, where M_w is the weight-average molecular weight of an entire block copolymer, w_K is the weight fraction of K-component, and $M_{u,K}$ is the molecular weight of K-segment. The value of $r_C = 1002$ which we reported in our previous paper[4] is not appropriate because we used the number-average molecular weight, M_n, instead of using M_w in the calculation of N_K values by mistake and the density value at 298 K was used for 1,4-polyisoprene[30] ($\rho_{PI} = 0.900$ g/cm^3). The reported value of $f_{PS} = 0.15$ in our previous paper[4] should be also corrected for by using the density value at 413 K for 1,4-polyisoprene[30] ($\rho_{PI} = 0.830$ g/cm^3).

(30) Fetters, L. J.; Lohse, D. J.; Richter, D.; Witten, T. A.; Zirkel, A. *Macromolecules* **1994**, *27*, 4639. Note for the statistical segment length: Small-angle neutron scattering (SANS) based $\langle R^2\rangle/M_w$ values in the melt yield slightly different statistical segment length, where $\langle R^2\rangle_0$ is mean squared unperturbed dimension of PS or PI. However, they compensate since $R_{g,SI} = 9.2$ nm. The independence of $R_{g,SI}$ with temperature is consistent with the SANS derived melt values for $d \ln \langle R^2\rangle_0/dT$ which is nearly zero for PS and ca. 0.4×10^{-3} deg^{-1} for PI.

(31) Bates, F. S.; Rosedale, J. H.; Fredrickson, G. H. *J. Chem. Phys.* **1990**, *92*, 6255.

(32) Duplessix, R.; Cotton, J. P.; Benoit, H.; Picot, C. *Polymer* **1979**, *20*, 1181.

(33) Mayes, A. M.; Barker, J. G.; Russell, T. P. *J. Chem. Phys.* **1994**, *101*, 5213.

(34) Mori, K.; Hasegawa, H.; Hashimoto, T. *Polymer* **1990** *31*, 2368.

(35) Hashimoto, T.; Shibayama, M.; Kawai, H. *Macromolecules* **1983** *16*, 1093. This paper shows $d \sim (\phi_p/T)^{1/3}$. $d \sim \chi_{eff}^{1/3}$ will be shown in a paper to be submitted. Mori, K.; Hashimoto, T., in preparation.

(36) The scheme illustrated in Figure 9 represents, of course, only a local event for the thermoreversible morphological transition between cylinders and spheres in the particular SI sample. We intend to present a picture in an initial stage of the morphological transition and do not intend to refer to subsequent ordering processes of microdomains. We believe this scheme represents one of the mechanisms, whereas many other possibilities may remain. To our best knowledge, no explicit experimental results have been published for the thermoreversible transition between cylinders and spheres. Koppi et al.[39] studied the transition between cylinders and spheres, although they used shear-oriented samples. They presented a possible scheme for the transition (Figure 3 in their paper) which is exactly the same as what we presented in our Figure 9. It is noteworthy that they also observed that the position for the first-order peaks is unchanged upon the cylinder−sphere transition.

(37) Owens, J. N.; Gancarz, I. S.; Koberstein, J. T.; Russell, T. P. *Macromolecules* **1989**, *22*, 3380.

(38) Bates, F. S.; Fredrickson, G. H. *Annu. Rev. Phys. Chem.* **1990**, *15*, 584.

(39) Koppi, K. A.; Tirrell, M.; Bates, F. S.; Almdal, K.; Mortensen, K. *J. Rheol.* **1994**, *38*, 999.

MA9502516